Available online at www.sciencedirect.com
SCIENCE DIRECT®
Developmental Biology 265 (2004) 127–139
DEVELOPMENTAL BIOLOGY
www.elsevier.com/locate/ydbio

The minibrain kinase homolog, *mbk-2*, is required for spindle positioning and asymmetric cell division in early *C. elegans* embryos

Ka Ming Pang,[a] Takao Ishidate,[a] Kuniaki Nakamura,[a] Masaki Shirayama,[a] Chris Trzepacz,[a] Charlotte M. Schubert,[b] James R. Priess,[b,c] and Craig C. Mello[a,c,*]

[a] *Department of Molecular Medicine, University of Massachusetts Medical School, Worcester, MA 01605, USA*
[b] *Department of Basic Science, Fred Hutchinson Cancer Research Center, Seattle, WA 98109, USA*
[c] *Howard Hughes Medical Institute, Chevy Chase, MD 20815, USA*

Received for publication 5 August 2003, revised 24 September 2003, accepted 24 September 2003

Abstract

In the newly fertilized *Caenorhabditis elegans* zygote, cytoplasmic determinants become localized asymmetrically along the anterior–posterior (A–P) axis of the embryo. The mitotic apparatus then orients so as to cleave the embryo into anterior and posterior blastomeres that differ in both size and developmental potential. Here we describe a role for MBK-2, a member of the Dyrk family of protein kinases, in asymmetric cell division in *C. elegans*. In *mbk-2* mutants, the initial mitotic spindle is misplaced and cytoplasmic factors, including the germline-specific protein PIE-1, are mislocalized. Our findings support a model in which MBK-2 down-regulates the katanin-related protein MEI-1 to control spindle positioning and acts through distinct, as yet unknown factors, to control the localization of cytoplasmic determinants. These findings in conjunction with work from *Schizosaccharomyces pombe* indicate a possible conserved role for Dyrk family kinases in the regulation of spindle placement during cell division.

Keywords: *mbk-2*; *pie-1*; P-granules; *mei-1*; Asymmetric division; Spindle orientation

Introduction

The *Caenorhabditis elegans* zygote undergoes a series of asymmetric divisions that exhibit well-defined polarity, timing, and outcome. This precisely orchestrated process depends on maternally expressed gene products that become localized along the anterior–posterior (A–P) axis of the embryo after fertilization. The PAR proteins PAR-1, PAR-2, PAR-3, PAR-6, and the atypical protein kinase C (PKC-3) protein compose conserved polarity regulators that act at an upstream step in this pathway (Kemphues, 2000; Pellettieri and Seydoux, 2002; Rose and Kemphues, 1998; Tabuse et al., 1998). Shortly after fertilization, the PAR-1 and PAR-2 proteins become localized at the posterior cortex of the egg while a complex consisting of PAR-3, PAR-6, and PKC-3 becomes localized at the anterior cortex. In response to the PAR proteins, MEX-5 and MEX-6, two highly homologous zinc finger proteins, localize to the anterior cytoplasm where they function via unknown mechanisms to regulate the A–P distribution of cytoplasmic and membrane-associated determinants such as the germline determinant PIE-1(Schubert et al., 2000).

Spindle positioning downstream of the PAR proteins requires a non-receptor-mediated heterotrimeric G-protein signaling cascade that appears to regulate the differences in force generation between the anterior and the posterior spindle poles, possibly through cortically anchored astral microtubules (Colombo et al., 2003; Gotta and Ahringer, 2001; Gotta et al., 2003; Grill et al., 2001; Srinivasan et al., 2003; Tsou et al., 2002). Additional genes that function in spindle placement appear to regulate the length of astral microtubules and thus ensure proper contact between the microtubules and the cortical signals that

* Corresponding author. Howard Hughes Medical Institute and Program in Molecular Medicine, University of Massachusetts Medical School, 373 Plantation Street, Worcester, MA 01605. Fax: +1-508-856-2950.
E-mail address: craig.mello@umassmed.edu (C.C. Mello).

0012-1606/$ - see front matter © 2003 Elsevier Inc. All rights reserved.
doi:10.1016/j.ydbio.2003.09.024

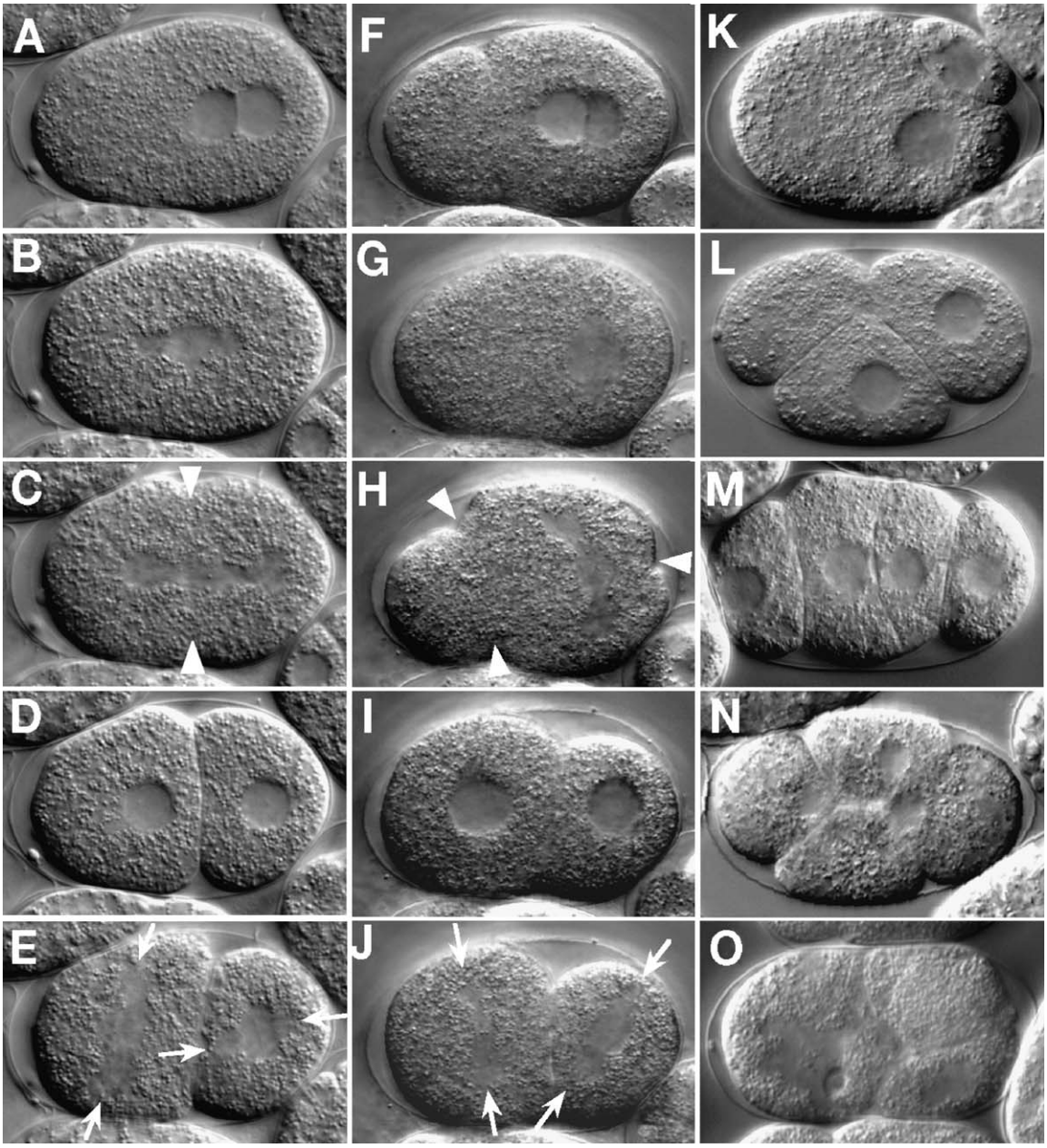

Fig. 1. MBK-2 is required for spindle positioning. DIC images showing sequences of early cell division in wild-type (A–E) and *mbk-2*(*ne992*) (F–J): pronuclear meeting (A and F); prometaphase (B and G); late anaphase (C and H); two-cell stage (D and I); anaphase of second division (E and J). Two-cell stage *mbk-2* embryos exhibiting daughter blastomeres of wild-type size (I), excessive asymmetric (K), and equal size with anterior cytoplast (L). Four-cell stage *mbk-2* embryo with liner array of daughter cells (M). *mbk-2* embryos undergoing tetrapolar cell division (N). Terminal *mbk-2* embryo with cytokinesis defects (O). Arrowheads in C and H indicate cleavage furrows. Arrows in E and J indicate the orientation of the spindles in the second mitotic division. All embryos in this and following figures are approximately 50 μm long and oriented with anterior to the left and posterior to the right.

direct spindle rotation and positioning. These latter genes include *mel-26* and *rfl-1*. MEL-26 is a conserved but poorly understood protein that contains one BTB and one MATH domain, which have been implicated in protein–protein interactions (Dow and Mains, 1998; Tsukuba and Bond, 1998; Zollman et al., 1994). RFL-1 is a member of the Uba3 family of E1-activating enzymes that interacts with the ubiquitin-like protein Nedd8. Genetic studies suggest that MEL-26 and RFL-1, along with additional components of the Nedd8 pathway, function to remove MEI-1, a homolog of the microtubule-severing protein katanin, after completion of meiosis (Dow and Mains, 1998; Kurz et al., 2002). Failure to remove MEI-1 after meiosis results in fragmented microtubules and failure of the astral microtubules to contact the cortex during the first mitotic division. The genetic removal of

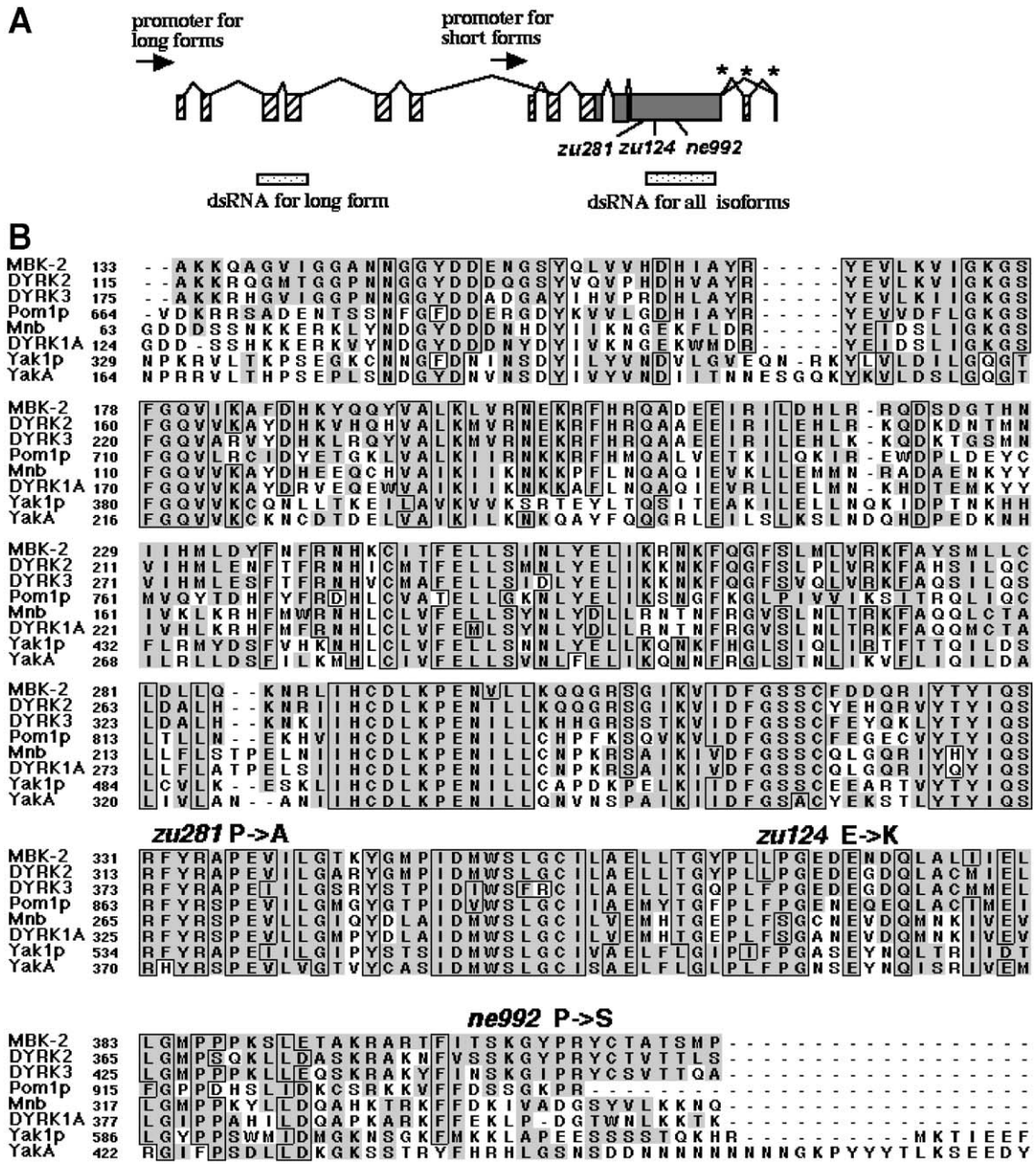

Fig. 2. The *mbk-2* locus. (A) Gene structure of *mbk-2*. Boxes represent exons. Filled boxes represent the predicted kinase domain. Asterisks represent stop codons. The last exon contains no coding sequence but only a TGA stop codon. Dotted bars represent regions used to make dsRNA for RNAi experiments. (B) Sequence alignment of the kinase domain of the Dyrk family proteins: MBK-2 of *C. elegans*; Dyrk1A, 2, and 3 of human; Pom1p of *S. pombe*; Minibrain (Mnb) of *D. melanogaster*; Yak1p of *S. cerevisiea*; YakA of *D. discoidium*. The lesions in the three alleles of *mbk-2* are indicated.

mei-1 activity can suppress the mitotic defects of both *mel-26* and *rfl-1* mutants.

Here we describe identification and characterization of three mutant alleles of *mbk-2*, which encodes a conserved member of the dual specificity and Yak1-regulated kinase (Dyrk) family of protein kinases, with homologs in yeast, insects, and vertebrates. All three mutant alleles, as well as RNAi targeting *mbk-2*, cause penetrant defects in the positioning of the first mitotic spindle and in the localization of germline-specific factors including the P-granules and the PIE-1 protein. The PAR-1, PAR-2, and PAR-3 proteins are properly localized in *mbk-2* mutant embryos, suggesting that MBK-2 functions downstream or independently of the PAR proteins to transduce polarity signals. Our genetic studies suggest that *mbk-2* is required along with MEL-26 and RFL-1 for the down-regulation of the microtubule-severing protein MEI-1/katanin and suggest that *mbk-2* regulates P-granule and PIE-1 protein locali-

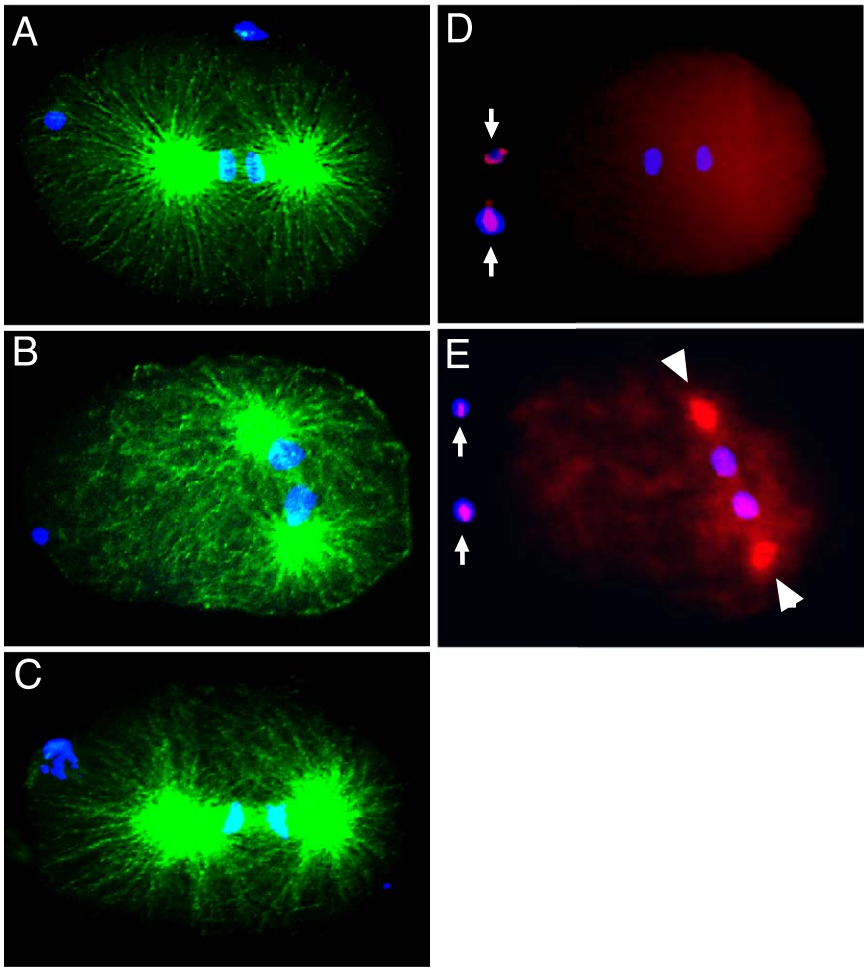

Fig. 3. MBK-2 negatively regulates MEI-1/katanin to stabilize microtubules. Indirect immunostaining of microtubules (green), MEI-1 (red), and DNA (blue) in wild-type (A and D), *mbk-2*(*ne992*) (B and E), and *mbk-2*(*ne992*); *mei-1*(RNAi) double mutants (C). Blue spots at the anterior of the embryos represent the polar bodies. Note the highly disorganized and fragmented microtubules in *mbk-2* mutant embryos (compare B to A). In wild-type embryos, MEI-1 is localized to the polar bodies only (arrows in D and E); but in *mbk-2* embryos, MEI-1 is also localized to the microtubules around the centrosomes (arrowheads in E). In the *mei-1* mutant embryo (C), meiotic daughter pronuclei fails to condense and therefore exhibit a larger DNA signal. All embryos are in the first mitotic anaphase.

zation through a distinct mechanism. Our studies along with previous work on the Pom1p kinase from *Schizosaccharomyces pombe* (Bahler and Nurse, 2001; Bahler and Pringle, 1998) demonstrate that MBK-2 is a conserved regulator of spindle positioning and suggest that it has multiple functions in transducing the polarity signals that direct asymmetric division in early *C. elegans* embryos.

Materials and methods

Strains and alleles

The Bristol strain N2 was used as the standard wild-type strain. *ne992* was isolated in the Hawaiian (CB4856) background. *zu124* and *zu281* were isolated in the N2 background. In addition, the following strains and genetic reagents were used: *mei-1*(*b284*); *mel-26*(*ct61*); MT464 [*unc-5*(*e53*)IV; *dpy-11*(*e224*)V; *lon-2*(*e678*)X]; MT465 [*dpy-5*(*e61*)I; *bli-2*(*e768*)II; *unc-32*(*e189*)III]; AZ235 (*unc-119*(ed3)III; ruIs48[*unc-119*(+) pie-1::tubulin::GFP fusion]); KK866 (itIs153, *pie-1::par-2::gfp::pie-1*); *dpy-4*(*e1166*); *dpy-20*(*e1282*); *unc-5*(*e53*); *unc-30*(*e191*). *C. elegans* culture and genetics were as described (Brenner, 1974). Strain expressing PIE-1::GFP was constructed by rescuing a pie-1(*zu127*) strain using a transgene made in YAC by homologous recombination as described (Rocheleau et al., 1999).

Isolation of the mbk-2 and mutant characterization

mbk-2(*zu124*) was isolated in a screen for strict maternal effect lethal mutants. *mbk-2*(*ne992*) was isolated in an F2 screen for temperature-sensitive embryonic lethal mutants. P0 *lin-11* Hawiian (CB4856) animals were

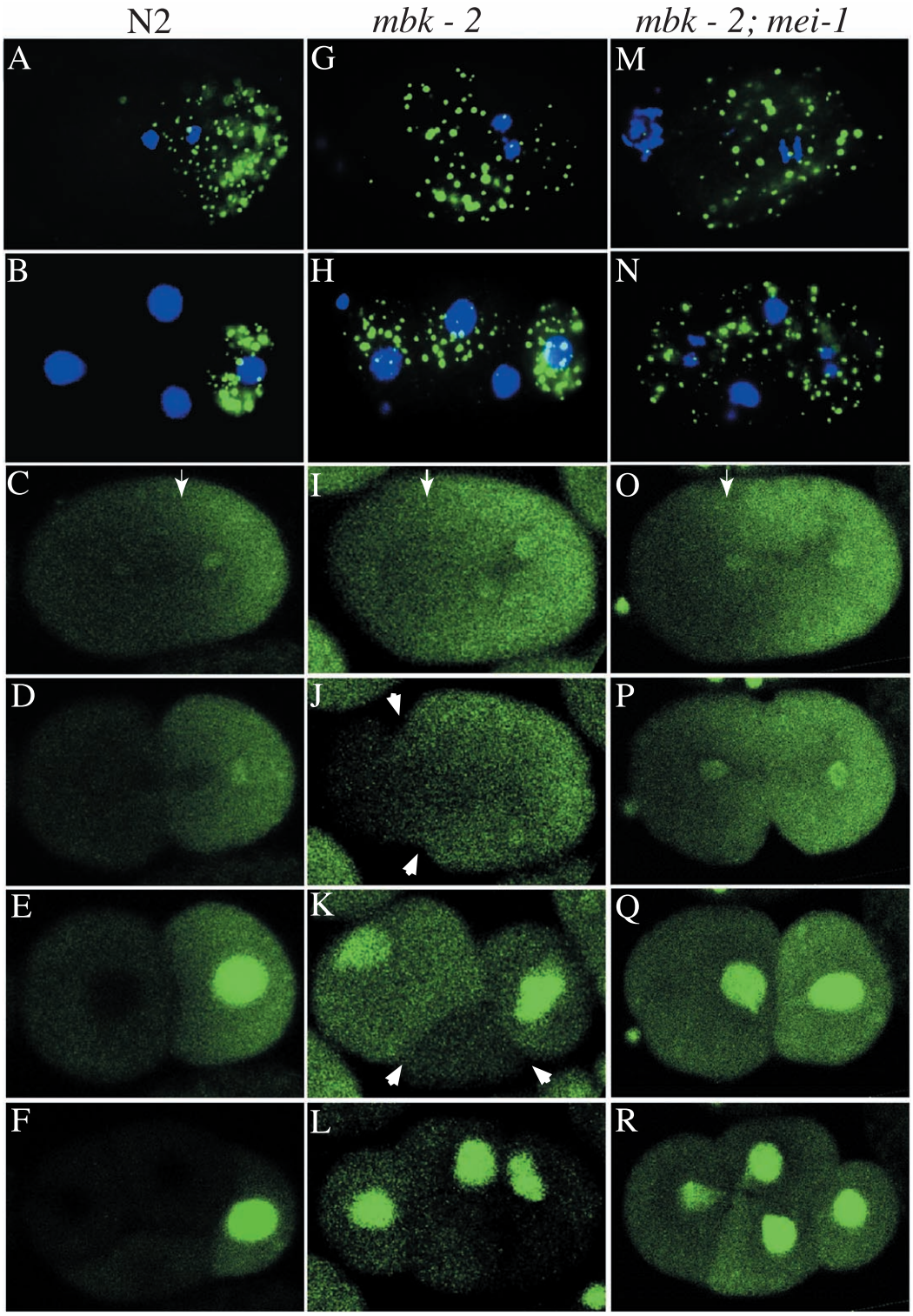

Fig. 4. MBK-2 is required for P-granule and PIE-1 localization. P-granules (green) and DNA (blue) staining in one-cell (A, G, and M) and four-cell (B, H, and N) embryos of wild-type (A and B), *mbk-2*(*ne992*) (G and H), and *mbk-2*(*ne992*); *mei-1*(RNAi) double mutants (M and N) are shown. Time sequences showing PIE-1 ::GFP in wild-type (C to F), *mbk-2*(RNAi) (I to L), and *mbk-2*(RNAi); *mei-1*(RNAi) (O to R) are shown. Comparable stages are shown: early anaphase (C, I, and O); late anaphase (D, J, and P); two-cell stage (E, K, and Q); and four-cell stage (F, L, and R). Arrows in panel C, I, and O mark the boundary of PIE-1 ::GFP localization in the one-cell embryos. Arrowheads in J mark anterior ectopic cleavage furrows. The anterior most cytoplasm in panel J is separated completely from the two daughter cells and is marked by arrowheads in panel K. All four daughter cells in panel L contain PIE-1 ::GFP signal; however, one daughter of the posterior cell is located slightly below the focal plane.

mutagenized by *N*-nitroso-*N*-ethylurea (ENU) or ethylmethanesulfonate (EMS). After growth at permissive temperature (15°C), the F2 L4 stage animals were shifted to 25°C for 27 h then downshifted to 15°C for 18 more h. The population is then briefly hypochlorited to kill all hatched larvae and adults so that dead embryos made at 25°C and viable embryos made after the shift down remain trapped together in the mothers uterus. The carcasses are then floated in 50% sucrose solution where adults filled with inviable or unhatched eggs remain floating in a band at the top. Candidate TS mutants were then identified by looking for viable L1 larvae bracketing a collection of dead eggs. Candidate mutants were retested for TS embryonic lethal and phenotypes analyzed. *mbk-2*(*zu281*) was isolated in a similar temperature-sensitive maternal effect lethal screen in N2 background. *ne992* was first located to individual chromosome by crossing to MT464 and MT465. Then three-factor mapping using first *unc-5* and *dpy-4* then *dpy-20* and *unc-30* were carried out to located *ne992* to about 7.6 map unit on chromosome IV. SNP mapping further located *ne992* to between SNPs on K10D11(position 1231) and F49E11(position 21006). *mbk-2* was identified by RNAi of candidate genes in the regions and confirmed by DNA sequencing.

Microinjection and molecular biology

RNAi was performed as described (Fire et al., 1998; Rocheleau et al., 1997). dsRNAs were made in vitro (Megascript T7 kit, Ambion) using PCR products containing T7 promoters in both primers as templates. Regions of the following genes were amplified from genomic DNA or cDNA: *mbk-2* (short form), amino acids 276-456; *mbk-2* (long form), amino acids 44-186; *mei-1*, full-length (yk786a08); *mei-2*, full-length (yk314c6).

Microscopy

In time-lapse video microscopy experiments, young adult animals were cut open in M9 solution and embryos were mounted on 2% agarose pads in M9 solution for recording. Time-lapse DIC images were collected by a Hamamatsu Ocre-ER digital camera mounted on a Zeiss Axioplan 2 under the control of Openlab 3.0 software. Stacks of images were edited by NIH Image 1.6 program (developed at the U.S. National Institutes of Health and available on the Internet http://rsb.info.nih.gov/nih-image/). In immunostaining experiments, antibodies against the following proteins were used as described: PGL-1 (Kawasaki et al., 1998), MEI-1/2 (Clark-Maguire and Mains, 1994), MEX-5 (Lin et al., 1995), PAR-1 (Guo and Kemphues, 1995), and PAR-3 (Etemad-Moghadam et al., 1995). Microtubules were stained with a monoclonal antitubulin antibody at 1:200 (YOL1/34, Accurate Chemical and Scientific Corp.), and DNA was stained with DAPI (4,6-diamidine-2-phenylindole-dihydrochoride, Roche Applied Science). Fluorescence images were collected using the same camera, microscope, and software as described above. Images collected were merged and enhanced by Photoshop 6 (Adobe System Inc.). Images of embryos expressing PIE-1::GFP and PAR-2::GFP were collected by Leica TCS SP2 confocal microscope system. In temperature upshift experiments, animals were cut open and embryos were put on pads preincubated at 15°C in a temperature-controlled room. The stages and early cell division patterns of the embryos were monitored by digital camera. These embryos were then put in wet chamber preincubated at 25°C and transferred to an adjacent temperature-controlled room set at 25°C for recording. Downshift experiments were performed in reverse order.

Results

mbk-2 is required for spindle positioning and cell fate determination in early C. elegans embryos

To identify genes required for cell-fate determination and cell polarity, we have conducted several large-scale screens for embryonic lethal mutants. Alleles of *mbk-2* were identified in two different genetic screens. One allele was identified in a screen for strict maternal-effect lethal mutants (Mello et al., 1992), while two alleles were identified in screens for temperature sensitive embryonic lethal mutants (see Materials and methods). All three alleles cause similar defects in which tissues differentiate properly but embryos arrest with abnormal and variable numbers of certain cell types. For example, 9% (n = 368) of *mbk-2*(*ne992ts*)-arrested embryos exhibited a total lack of endoderm while 11% of the arrested embryos produce nearly twice the normal complement of intestinal cells.

The terminal-arrest phenotype of the *mbk-2* mutant embryos was similar in some respects to the phenotypes caused by mutants that disrupt early cell division patterns. We therefore used time-lapse video microscopy to analyze early cell divisions in *mbk-2* mutants. In wild-type embryos, the maternal pronucleus migrates to the posterior where it meets the paternal pronucleus. The nuclei then migrate to the center of the embryo, the centrosomes rotate 90° so that the mitotic spindle becomes aligned along the longitudinal axis (anterior–posterior axis). During the first cell division in wild-type embryos, the mitotic apparatus exhibits a slight posterior displacement such that the chromosomes align during metaphase at approximately 55% ± 5.3% (n = 13) of the length of the embryo. During anaphase, the posterior centrosome undergoes a rocking motion and the spindle is further displaced towards the posterior pole, ultimately resulting in a larger anterior and a smaller posterior cell (Figs. 1A–D). In the second division, the anterior AB cell

divides transversely while the posterior P1 cell divides longitudinally (Fig. 1E). In *mbk-2* mutants, the maternal pronucleus migrates to the posterior and meets the paternal pronucleus, as observed in wild-type embryos (Fig. 1F). However, the pronuclei do not migrate to the center of the embryo and the centrosomes do not rotate (Fig. 1G). During metaphase of the first cell-cycle, the zygotic nucleus is positioned at 71% ± 5.4% (n = 23) of embryo length, and in 100% of the embryos, the mitotic spindle aligns transversely to the anterior–posterior (A–P) axis (Fig. 1H). During cytokinesis, multiple cleavage furrows form: one circumferential furrow forms at the anterior of the embryo; a second furrow forms at the posterior end of the embryo, perpendicular to the spindle (arrowheads in Fig. 1H). Both furrows ingress and in most embryos the posterior furrow ultimately intersects with the anterior furrow to cleave the embryo into two cells that can vary widely in size, from approximately wild type (68%, n = 25; Fig. 1I) to excessively asymmetric (8%; Fig. 1K). In 12% of the embryos analyzed, the anterior furrow cleaves the embryo to produce an anterior cytoplast and a posterior cell, which also completes cytokinesis to produce two small posterior daughter cells (Fig. 1L).

In the second cell division, the majority of the embryos analyzed (64%) produced daughter cells that divided transversely to the A–P axis (Fig. 1J). While in 24% of the embryos, the spindles of both daughter cells aligned along the A–P axis to produce a linear array of cells at the four-cell stage (Fig. 1M). The remaining 12% of embryos analyzed failed to divide during the first division and underwent a tetrapolar division to generate four cells during the second division (Fig. 1N). The average time from pronuclear fusion to the end of first and second mitotic divisions was similar to that observed in wild-type embryos (data not shown). However, at the second division, daughter blastomeres divided synchronously in most mutant embryos (94%, n = 18) instead of asynchronously as in wild type (100%, n = 10). Both the terminal phenotype and the cell division phenotypes described above were similar for all three *mbk-2* mutant strains. However, a higher percentage of the RNAi embryos (60%, n = 20) failed to complete cytokinesis, resulting in large multinucleated cells (Fig. 1O).

mbk-2 functions primarily during the first division

To determine when *mbk-2* activity is required during embryogenesis, we performed a series of temperature-shift experiment on early embryos. The *mbk-2*(*ne992ts*) mutant embryos were acutely sensitive to temperature shift, exhibiting a change from the wild-type division pattern to the *mbk-2* division pattern within 1 min after upshift. All of the *mbk-2*(*ne992ts*) embryos that were upshifted during the one-cell stage exhibited a spectrum of terminal arrest phenotypes similar to those observed in embryos cultured continuously at nonpermissive temperature (data not shown). In contrast, when cultured at permissive temperature until the two-cell stage and then shifted up to nonpermissive temperature, approximately 50% (n = 30) of the embryos survived to hatching. The proportion of viable embryos increased to nearly 100% when embryos were shifted up to nonpermissive temperature after the eight-cell stage (n = 24). Downshift experiments resulted in a reciprocal outcome; all embryos (n = 94) downshifted after the first division arrested development, indicating that *mbk-2* activity is required during the first mitotic division and that its continued activity may contribute, albeit less critically, at later stages.

mbk-2 encodes a putative kinase of the Dyrk family

To identify the *mbk-2* gene, we used visible markers to map the gene to a small genetic interval on chromosome IV. Single nucleotide polymorphisms (SNPs) were then used to map the gene to cosmid F49E11 (see Materials and methods). RNAi of candidate genes within this region revealed that F49E11.1 exhibits an RNAi phenotype very similar to that of the *mbk-2* mutants. DNA sequencing confirmed that each allele of *mbk-2* contains a single point mutation in the predicted open reading frame of F49E11.1 (Fig. 2). Sequencing of cDNA clones confirmed the structures of the F49E11.1a, b, and c isoforms predicted by the genome consortium. However, RNAi targeting the predicted long isoforms failed to induce a phenotype, suggesting that this predicted longer isoform is either not produced or is not essential for *mbk-2* function in the embryo (data not shown). We also detected several alternative isoforms not predicted by Wormbase that result from alternative splicing at the 3′ end of the gene (Fig. 2A). F49E11.1 corresponds to a previously identified gene minibrain kinase 2 (*mbk-2*), a homolog of the human gene Dyrk and the *S. pombe* gene *pom1* (Raich et al., 2003). All three of our mutant alleles contained lesions in the putative kinase domain, suggesting that the kinase activity may be important for MBK-2 function.

Microtubule organization is defective in mbk-2 embryos

The spindle placement and orientation defects of *mbk-2* mutant embryos are similar to those observed previously for several genes required for microtubule stability, including *mel-26* and *rfl-1*, and are also similar to the defects caused by treating embryos with the microtubule destabilizing drug nocodozole (Dow and Mains, 1998; Kurz et al., 2002). Therefore, we asked whether *mbk-2* embryos have microtubule defects. We found that the microtubules in one cell *mbk-2*(*ne992*) mutant (n = 21; Fig. 3B) or *mbk-2*(RNAi) embryos (n = 20, data not shown) appeared shorter and less well organized, with fewer microtubules extending to the cortex when compared to wild-type embryos (Fig. 3A). There were also numerous apparent fragments of microtubules observed throughout the embryos, especially in the anterior region of the embryo (Fig. 3B).

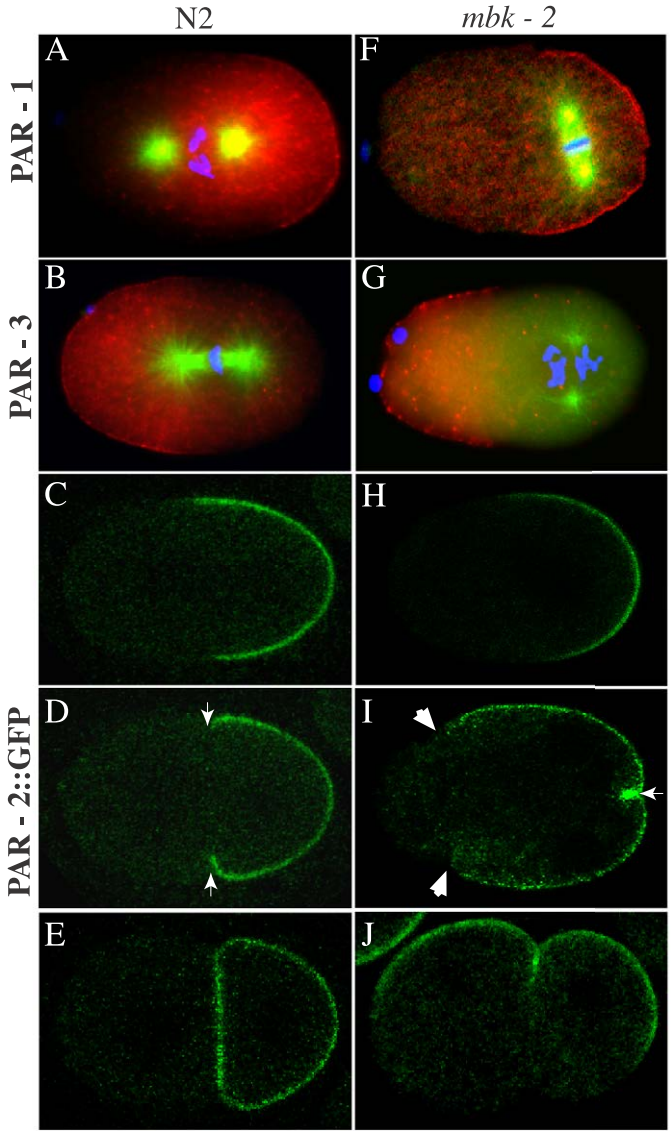

Fig. 5. Localization of PAR-1, PAR-2, and PAR-3 in *mbk-2* mutant embryos. Immunostaining of PAR-1 (red in A and F) and PAR-3 (red in B and G) in one-cell stage wild-type (A and B) and *mbk-2*(*ne992*) mutants (F and G). Microtubules (green) and DNA (blue) are also shown. PAR-2::GFP localization in wild-type (C to E) and *mbk-2*(RNAi) (H to J) live embryos of the following stages: metaphase (C and H); late anaphase (D and I); and two-cell stage (E and J). Arrows in panel D and I mark the cleavage furrow that bisects the spindles. Arrowheads in panel I mark the anterior ectopic cleavage furrow that coincides with the boundary of PAR-2::GFP localization.

This defect in the organization of microtubules could reflect either a failure to promote microtubule growth or increased turnover or severing of microtubules. Previous studies have shown that the inappropriate activity of MEI-1, which is related to the microtubule-severing protein katanin, underlies the microtubule defects observed in the mutant *mel-26* and *rfl-1* (Dow and Mains, 1998; Kurz et al., 2002). In wild-type animals, MEI-1 associates with the meiotic spindles and is required for the completion of meiosis. However, MEI-1 disappears shortly after fertilization in the wild-type zygote, possibly due to protein degradation. To ask if MEI-1 protein persists inappropriately after fertilization in *mbk-2* mutants, we used a MEI-1-specific antibody to stain one-cell stage *mbk-2* mutant embryos. We found that, in both *mbk-2*(*ne992ts*) (n = 22) and *mbk-2*(RNAi) (n = 25) embryos, MEI-1 protein persists at high levels around the centrosomes (Fig. 3E and data not shown). These results suggest that MBK-2 functions to down-regulate MEI-1 protein levels before the onset of mitosis. To ask if the *mbk-2* phenotype is caused by the ectopic accumulation of MEI-1, we constructed double mutants. In several different double mutant combinations, including *mbk-2*(*ne992ts*);*mei-1*(RNAi), *mbk-2*(RNAi);*mei-1*(RNAi), and *mbk-2*(RNAi);*mei-1*(*b284*), 100% of the embryos from each double mutant combination exhibited proper spindle placement and orientation during the first two mitotic divisions (Table 1). Moreover, the organization of the microtubule network was restored in the double mutant (Fig. 3C). Since

MEI-1 requires MEI-2 for proper localization (Srayko et al., 2000), we also examined the spindle orientation in *mbk-2*(*ne992ts*);*mei-2*(RNAi) mutant embryos. We found that a lower percentage of *mbk-2*(*ne992ts*);*mei-2*(RNAi) embryos exhibited proper spindle placement and division pattern (Table 1), consistent with a less crucial role for MEI-2. Taken together, these findings suggest that MBK-2 is required to ensure low levels of MEI-1 protein before the onset of the first mitotic division.

mbk-2 is required for proper localization of P-granules and the PIE-1 protein

The cell-fate defects associated with *mbk-2* mutants could stem from the mislocalization of cytoplasmic determinants during the early divisions. We therefore asked whether P-granules and the PIE-1 protein, which are normally restricted to the posterior before the first division (Figs. 4A and C), are mislocalized in *mbk-2* mutants. We used the K76 monoclonal antibody to follow P-granule localization and a rescuing PIE-1::GFP fusion protein to follow PIE-1 protein localization. All of the mutant embryos examined (n = 30) exhibited abnormally high levels of P-granules and PIE-1::GFP protein in the anterior cytoplasm at the one-cell stage (Figs. 4G and I).

Using the PIE-1::GFP marker, we were able to view the dynamics of PIE-1 mislocalization. After fertilization, PIE-1::GFP began to localize to the posterior of the embryo coincident with the migration of the maternal pronucleus. However, the extent of posterior localization was less than that of the wild type. For wild-type embryos, PIE-1::GFP was localized to the posterior-most 40% of the one-cell embryo (n = 7), while in *mbk-2*(RNAi) embryos PIE-1::GFP was excluded only from the anterior-most 30% to 40% of the embryo and was diffusely localized throughout the remaining region (n = 9) (Fig. 4, compare G and I with A and C). During cytokinesis, PIE-1::GFP was divided by ingression of the posterior cleavage furrow and became localized to both daughter cells (Figs. 4K and L). The cytoplasm anterior to the ectopic cleavage furrow exhibited very low levels of PIE-1::GFP suggesting that a mechanism required for PIE-1 localization remains intact in the anterior-most region of the embryo (Figs. 4J and K).

Since mislocalization of both the P-granules and PIE-1 protein was apparent before the first division, we reasoned that although the misalignment of the first mitotic spindle clearly contributes to mislocalization of these factors, it was unlikely to be entirely responsible. We therefore examined localization of PIE-1 and P-granules in double mutants with *mei-1* in which spindle alignment is restored to the wild-type orientation. We found that although *mei-1* mutants fully restore proper spindle placement and orientation as described above, they do not restore proper P-granule or PIE-1 localization caused by *mbk-2* (n = 9; Figs. 4M, N, P–R). In contrast, although *mel-26* and *rfl-1* both exhibit *mei-1* suppressible spindle placement defects that are very similar to those described here for *mbk-2* (Dow and Mains, 1998; Kurz et al., 2002), we did not observe mislocalization of P-granules or of PIE-1::GFP protein in one-cell embryos from these mutant backgrounds. Furthermore, in double mutants with *mei-1*, we found that *mel-26* and *rfl-1* mutant embryos not only exhibited proper spindle positioning but also exhibited proper localization of both P-granules (n = 30 and 25, respectively) and of PIE-1 protein (n = 20 and 22, respectively). Taken together, these findings suggest that MBK-2 differs from MEL-26 and RFL-1 in that it is required to regulate not only MEI-1 and hence spindle placement, but is also required to regulate the localization of cytoplasmic factors in the early embryo.

Table 1
Suppression of *mbk-2* spindle orientation defects by *mei-1*

	Percentage with normal pattern of first two mitotic divisions	n
mbk-2(*ne992*); *mei-1*(RNAi)	100	(23/23)
mbk-2(*zu124*); *mei-1*(RNAi)	100	(14/14)
mei-1(*b284*); *mbk-2*(RNAi)	100	(8/8)
mbk-2(*ne992*); *mei-2*(RNAi)	67	(6/9)

MBK-2 is not required for the initial anterior-posterior asymmetries

The MEX-5 protein localizes to the anterior of the one-cell embryo and is required for the posterior localization of both P-granules and PIE-1(Schubert et al., 2000). Conceivably, MBK-2 could act through MEX-5 or could be required for the expression or localization of MEX-5. We therefore asked if MEX-5 protein is expressed and properly localized in *mbk-2* mutants. We found that MEX-5 was localized to the anterior cytoplasm of one-cell *mbk-2* mutant embryos with a pattern identical to wild-type embryos (data not shown). Although MEX-5 was mislocalized in the two- or four-cell *mbk-2* embryos, this mislocalization was fully suppressed by *mei-1*(RNAi), suggesting that the defects in MEX-5 localization are a secondary consequence of the improper cleavage planes in *mbk-2* mutant embryos.

We next asked if the polarity markers PAR-1, PAR-2, and PAR-3 are properly localized in *mbk-2* mutants. In wild-type embryos, PAR-1 and PAR-2 localize to the posterior cortex in the one-cell embryo and are localized to the cortex of the posterior daughter cell in two-cell embryos (Figs. 5A, C, and E). Conversely, PAR-3 localizes to the anterior cortex in one-cell embryos and to the cortex of the anterior cell in two-cell embryos (Fig. 5B and not shown). We found that during the one-cell stage in *mbk-2* mutant embryos, the localization of PAR-1 (n = 20), PAR-2 (n = 8), and PAR-3 (n = 23) was similar to that observed in wild-type embryos (Figs. 5F–H). However, these proteins became mislocalized during the two-cell stage (Fig. 5J and data not shown). To follow the dynamics of PAR-2 localization, we used a PAR-2::GFP (Wallenfang and Seydoux, 2000) to monitor cell

divisions in *mbk-2*(RNAi) embryos. We found that PAR-2::GFP was localized properly to the posterior of the embryo before the onset of the first mitotic anaphase ($n = 8$; Fig. 5H). However, during anaphase, PAR-2::GFP began to extend toward the anterior to the point where the ectopic cleavage furrows were observed (Figs. 5I and 1H). Also, the posterior furrow started to ingress and bisected the cortex marked by PAR-2::GFP. As a result, PAR-2::GFP localized to both the anterior and the posterior daughter cells (Fig. 5J). Since PAR-2 is required to restrict the localization of PAR-3 to the anterior cortex and to mark the area for PAR-1 localization, it is likely that PAR-1 and PAR-3 mislocalization at the two-cell stage both result from the improper spindle and cleavage furrow placement.

At anaphase, the boundary of PAR-2::GFP localization was displaced anteriorly relative to its wild-type position in the *mbk-2* embryos (compare Figs. 5D and I). We wondered if this displacement was caused indirectly by misplacement of the spindle. To address this possibility, we monitored localization of PAR-2::GFP in *mbk-2*(*ne992ts*); *mei-1*(RNAi) ($n = 8$) or *mbk-2*(RNAi);*mei-1*(RNAi) ($n = 6$) double mutant embryos. We found that in the double mutants, the PAR-2::GFP localization pattern was indistinguishable from that of wild-type (data not shown), suggesting that the anterior displacement of PAR-2 was caused indirectly by the misplaced microtubule network.

Discussion

Here we have described the genetic identification and characterization of three mutant alleles of the *C. elegans mbk-2* gene. MBK-2 is a member of the Dyrk family of protein kinases, with homologs in yeast, insects, and vertebrates. These homologs include the mammalian Dyrks, minibrain of *Drosophila*, Pom1p of *S. pombe*, Yak1p of *Saccharomyces cerevisiae*, and YakA of *Dictyostelium* (Bahler and Pringle, 1998; Garrett and Broach, 1989; Kentrup et al., 1996; Souza et al., 1998; Tejedor et al., 1995). In *Drosophila*, Minibrain (Mnb) is involved in postembryonic neurogenesis, regulating the size of optic lobes and brain hemispheres (Tejedor et al., 1995). The mammalian ortholog of Mnb, Dyrk1A, is required for proper neurodevelopment in mouse (Altafaj et al., 2001; Fotaki et al., 2002). In humans, overexpression of Dyrk1A, which resides on chromosome 21, may be linked to the neurological defects associated with Down syndrome (Smith et al., 1997).

In unicellular eukaryotes, Dyrk family members have been implicated in cell cycle control and transition from growth to development (Bahler and Nurse, 2001; Garrett et al., 1991; Souza et al., 1998). For example, in *S. pombe*, the kinase activity of Pom1p is cell-cycle regulated and *pom1* mutants exhibit defects in the placement of the mitotic spindle, cleavage furrow, and septum (Bahler and Nurse, 2001; Bahler and Pringle, 1998). In *C. elegans*, there are three members of this family, *mbk-1*, *mbk-2*, and *hpk-1* (Raich et al., 2003). The overexpression of MBK-1 causes defects in chemotaxis. However, no obvious defects in neuronal function were observed in *mbk-1* and *hpk-1* RNAi studies (Raich et al., 2003). Although a null maternal effect lethal allele of *mbk-2* was generated in this previous study, the lethal phenotype was not analyzed (Raich et al., 2003). Our characterization of three *mbk-2* alleles and of *mbk-2*(RNAi) phenotypes in *C. elegans* implicate MBK-2 in the proper positioning of the first mitotic spindle and in the localization of cytoplasmic determinants.

MBK-2 and asymmetric division

Asymmetric cell division is a fundamental mechanism for generating different cell types in metazoan development. In addition to the differential localization of cytoplasmic and cortical determinants along one axis of the cell, asymmetric cell division requires that the mitotic apparatus align with the polarized axis, such that cell division generates daughters that inherit distinct developmental determinants. Here we have identified the gene, *mbk-2*, which is required for proper asymmetric division of the fertilized *C. elegans* embryo. We have shown that MBK-2 activity is required for at least two distinct processes: First, MBK-2 is required for the proper positioning and orientation of the initial mitotic spindle; and second, MBK-2 is required to ensure the proper asymmetric distribution of the P-granules and of the PIE-1 protein in daughter cells.

In *S. pombe*, the MBK-2 homolog, Pom1p, is required for positioning the mitotic spindle to ensure symmetric cell division. Thus, the mutant phenotypes of *pom1* and *mbk-2* both include mispositioning of the mitotic spindle. However, the underlying cytoskeletal defects appear to be nearly opposite in these two organisms. In *mbk-2* mutants, the microtubules are short and appear fragmented. In contrast, in *pom1* mutants the microtubules are long and curved. Furthermore, when *pom1* is overexpressed in *S. pombe*, the microtubules appeared shorter and aberrant (Bahler and Pringle, 1998). From these studies, it is clear that both MBK-2 and Pom1p regulate microtubule stability. However, the sign of regulation appears to be opposite, while it is possible that these phenotypic effects are purely coincidental and do not reflect a conserved role for these proteins in regulating spindle positioning. It is also possible that these kinases share a conserved target required for the regulation of microtubule stability but have acquired divergent affects on the activity of the target protein or protein complex. We have shown that the fragmented microtubules observed in *mbk-2* mutants result from the persistent expression of a microtubule-severing, katanin homolog, MEI-1. Thus, it will be interesting to learn if the microtubule stability defects associated with *pom-1* might also result from misregulation of a katanin.

Although the direct targets for MBK-2 are not yet known, our genetic studies suggest several potential targets.

Before the first division, MBK-2 appears to function along with the conserved BTB-domain protein MEL-26 and the Nedd8/RFL-1 pathway to negatively regulate MEI-1. While the function of MEL-26 is not clear, the Nedd8 pathway has been shown to transfer the ubiquitin-like peptide Nedd8 onto target proteins, which typically are cullins, components of the SCF ubiquitin pathway for protein degradation. Consistent with this idea, *C. elegans* CUL-3 has been implicated in down-regulating MEI-1, suggesting that the Nedd8 pathway may activate CUL-3 for MEI-1 proteolysis (Kurz et al., 2002; Pintard et al., 2003). Thus conceivably, MBK-2 could act directly on MEI-1, perhaps phosphorylating it to prime its recognition by a CUL-3-dependent ubiquitin proteolysis pathway. Alternatively, MBK-2 could act indirectly through MEL-26 or components of the SCF complex to target MEI-1 for degradation (Fig. 6).

The function of MBK-2 in controlling the localization of P-granules and PIE-1 may also involve directed proteolysis. The genes that encode P-granule components and PIE-1 are maternally expressed, and their protein products but not their mRNAs are restricted to the germline descendant after each of several asymmetric divisions. For PIE-1, the mechanism of localization has been the subject of several studies and appears to involve a combination of directed localization of the protein and subsequent degradation of any PIE-1 protein remaining in the somatic sister cells after each division (Reese et al., 2000). The MEX-5 protein, a PIE-1 homolog, is a key regulator of PIE-1, the P-granules, and several other asymmetrically localized proteins (Schubert et al., 2000). Although its mode of action is unknown, it has been suggested that MEX-5 may promote the destruction of PIE-1 and other proteins in the anterior blastomere at the two-cell stage (Cuenca et al., 2003; Schubert et al., 2000). We found that the MEX-5 protein exhibits a wild-type distribution in *mbk-2* mutant embryos (data not shown), indicating that MBK-2 does not control the anterior localization of MEX-5. Therefore, MBK-2 could act in parallel with MEX-5 or could function upstream to stimulate its activity or downstream to promote MEX-5-dependent degradation of the P-granules and PIE-1 (Fig. 6).

However, our findings indicate that the pathway that regulates P-granule and PIE-1 protein localization appears to be distinct from the MEL-26, RFL-1 pathway that targets MEI-1. Thus, for example, if MBK-2-dependent phosphorylation triggers the MEL-26 and RFL-1-dependent SCF substrate-recognition process for MEI-1, then the degradation of PIE-1 and P-granule components may depend on other proteins related to, but distinct from, MEL-26 and RFL-1. Consistent with this idea, a recent study indicated that a complex containing a SOCS-box protein, CUL-2 and UBC-5, is specifically required for the degradation of several germline zinc finger proteins including PIE-1, POS-1, and MEX-5/6 but not for degradation of other germline proteins such as PAR-2 and PGL-1 (DeRenzo et al., 2003). *C. elegans* contains at least 35 *mel-26*-related genes, 5 *rfl-1*-related *uba* genes, and 20 *ubc* genes (Jones et al., 2002). Interestingly, RNAi experiments indicate that four of the *uba* genes and five of the *ubc* genes confer embryonic lethality (Jones et al., 2002). It will be interesting to investigate whether and how *mbk-2* functions in these distinct protein degradation pathways.

Our studies suggest that MBK-2 plays a critical role in coordinating the positioning of the cleavage furrow with respect to asymmetrically localized determinants. On one hand, by down-regulating the katanin homolog MEI-1, the MBK-2 protein ensures that astral microtubules contact cortical signals that may direct the positioning of the mitotic apparatus onto the polarized axis of the embryo. On the other hand, MBK-2 functions in the asymmetric localization of the P-granules and PIE-1 protein. However, in *mbk-2* mutant embryos, the asymmetric localization of upstream cortical factors (the PAR proteins) is unperturbed, and a small anterior region appears to be cleared of PIE-1::GFP before cytokinesis, suggesting that MBK-2 is not absolutely required for the initial asymmetric localization of determinants. Rather, MBK-2 appears to be required for defining the anterior boundary of PIE-1 protein and the P-granules. These activities may help to insure that the localization of these cytpolasmic factors coincides with the boundary of asymmetrically localized cortical factors, such as PAR-2, and with the approximate position of the cleavage furrow. Thus, understanding how MBK-2 functions should shed light on the mechanisms that coordinate the localization of cortical and cytoplasmic factors both with each other and with respect to the position of the cleavage furrow; mechanisms that at present remain almost entirely mysterious.

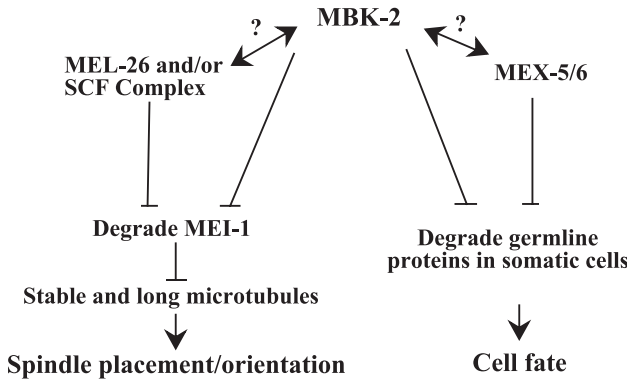

Fig. 6. Model for MBK-2 function in early *C. elegans* embryos. Schematic representation of possible regulatory interactions between MBK-2 and other proteins involved in asymmetric cell division. The genetic data indicate that *mbk-2* down-regulates MEI-1 protein levels to control spindle orientation in the one-cell embryo and similarly down-regulates PIE-1 and P-granules in the anterior daughter cell (bars extending to these targets). We cannot order the activity of *mbk-2* with respect to *mel-26*/SCF or *mex-5/6* because the corresponding mutants have phenotypes similar to *mbk-2*. We have tentatively placed MBK-2 upstream of both pathways because it exhibits a more pleiotropic effect. However, it is also possible that MBK-2 functions downstream or in parallel (indicated by the double-headed arrows with question marks).

In summary, the findings described here indicate that MBK-2 functions in both spindle positioning and in the localization of cytoplasmic determinants in early *C. elegans* embryos. These findings suggest that Dyrk family kinases may be conserved regulators of microtubule stability and spindle placement and provide the first evidence linking this family of kinases to asymmetric cell division. Understanding the biochemical and cell-biological mechanisms underlying MBK-2 action may provide insights into how other Dyrk family kinases function in cell division, nervous system development, and possibly in Down syndrome.

Acknowledgments

The authors would like to thank Tae-Ho Shin and members of the laboratory for helpful discussion and comments on the manuscript. In addition, we thank Paul Mains, Ken Kemphues, and Susan Strome for providing antibodies; Alan Coulson and Yoji Kohara for providing YAC and cDNA clones; and the *C. elegans* Genetics Center (funded by the NIH National Center for Research Support) for providing strains. Research support was provided in part by an NIH grant (HD36247) to C.C.M. C.C.M is a Howard Hughes Medical Institute assistant investigator. K.M.P. was supported by NIH postdoctoral fellowship (GM20795) and The Charles A. King Trust and The Campbell and Hall Charity Fund (Boston, MA).

References

Altafaj, X., Dierssen, M., Baamonde, C., Marti, E., Visa, J., Guimera, J., Oset, M., Gonzalez, J.R., Florez, J., Fillat, C., Estivill, X., 2001. Neurodevelopmental delay, motor abnormalities and cognitive deficits in transgenic mice overexpressing Dyrk1A (minibrain), a murine model of Down's syndrome. Hum. Mol. Genet. 10, 1915–1923.

Bahler, J., Nurse, P., 2001. Fission yeast Pom1p kinase activity is cell cycle regulated and essential for cellular symmetry during growth and division. EMBO J. 20, 1064–1073.

Bahler, J., Pringle, J.R., 1998. Pom1p, a fission yeast protein kinase that provides positional information for both polarized growth and cytokinesis. Genes Dev. 12, 1356–1370.

Brenner, S., 1974. The genetics of *Caenorhabditis elegans*. Genetics 77, 71–94.

Clark-Maguire, S., Mains, P.E., 1994. Localization of the *mei-1* gene product of *Caenorhaditis elegans*, a meiotic-specific spindle component. J. Cell Biol. 126, 199–209.

Colombo, K., Grill, S.W., Kimple, R.J., Willard, F.S., Siderovski, D.P., Gonczy, P., 2003. Translation of polarity cues into asymmetric spindle positioning in *Caenorhabditis elegans* embryos. Science 300, 1957–1961.

Cuenca, A.A., Schetter, A., Aceto, D., Kemphues, K., Seydoux, G., 2003. Polarization of the *C. elegans* zygote proceeds via distinct establishment and maintenance phases. Development 130, 1255–1265.

Dow, M.R., Mains, P.E., 1998. Genetic and molecular characterization of the *Caenorhabditis elegans* gene, *mel-26*, a postmeiotic negative regulator of *mei-1*, a meiotic-specific spindle component. Genetics 150, 119–128.

DeRenzo, C., Reese, K.J., Seydoux, G., 2003. Exclusion of germ plasm proteins from somatic lineages by cullin-dependent degradation. Nature 424, 685–689.

Etemad-Moghadam, B., Guo, S., Kemphues, K.J., 1995. Asymmetrically distributed PAR-3 protein contributes to cell polarity and spindle alignment in early *C. elegans* embryos. Cell 83, 743–752.

Fire, A., Xu, S., Montgomery, M.K., Kostas, S.A., Driver, S.E., Mello, C.C., 1998. Potent and specific genetic interference by double-stranded RNA in *Caenorhabditis elegans*. Nature 391, 806–811.

Fotaki, V., Dierssen, M., Alcantara, S., Martinez, S., Marti, E., Casas, C., Visa, J., Soriano, E., Estivill, X., Arbones, M.L., 2002. Dyrk1A haploinsufficiency affects viability and causes developmental delay and abnormal brain morphology in mice. Mol. Cell. Biol. 22, 6636–6647.

Garrett, S., Broach, J., 1989. Loss of Ras activity in *Saccharomyces cerevisiae* is suppressed by disruptions of a new kinase gene, YAKI, whose product may act downstream of the cAMP-dependent protein kinase. Genes Dev. 3, 1336–1348.

Garrett, S., Menold, M.M., Broach, J.R., 1991. The *Saccharomyces cerevisiae* YAK1 gene encodes a protein kinase that is induced by arrest early in the cell cycle. Mol. Cell. Biol. 11, 4045–4052.

Gotta, M., Ahringer, J., 2001. Distinct roles for Galpha and Gbetagamma in regulating spindle position and orientation in *Caenorhabditis elegans* embryos. Nat. Cell Biol. 3, 297–300.

Gotta, M., Dong, Y., Peterson, Y.K., Lanier, S.M., Ahringer, J., 2003. Asymmetrically distributed *C. elegans* homologs of AGS3/PINS control spindle position in the early embryo. Curr. Biol. 13, 1029–1037.

Grill, S.W., Gonczy, P., Stelzer, E.H., Hyman, A.A., 2001. Polarity controls forces governing asymmetric spindle positioning in the *Caenorhabditis elegans* embryo. Nature 409, 630–633.

Guo, S., Kemphues, K.J., 1995. par-1, a gene required for establishing polarity in *C. elegans* embryos, encodes a putative Ser/Thr kinase that is asymmetrically distributed. Cell 81, 611–620.

Jones, D., Crowe, E., Stevens, T.A., Candido, E.P., 2002. Functional and phylogenetic analysis of the ubiquitylation system in *Caenorhabditis elegans*: ubiquitin-conjugating enzymes, ubiquitin-activating enzymes, and ubiquitin-like proteins. Genome Biol. 3, 2.1–2.15 (Research).

Kawasaki, I., Shim, Y.H., Kirchner, J., Kaminker, J., Wood, W.B., Strome, S., 1998. PGL-1, a predicted RNA-binding component of germ granules, is essential for fertility in *C. elegans*. Cell 94, 635–645.

Kemphues, K., 2000. PARsing embryonic polarity. Cell 101, 345–348.

Kentrup, H., Becker, W., Heukelbach, J., Wilmes, A., Schurmann, A., Huppertz, C., Kainulainen, H., Joost, H.G., 1996. Dyrk, a dual specificity protein kinase with unique structural features whose activity is dependent on tyrosine residues between subdomains VII and VIII. J. Biol. Chem. 271, 3488–3495.

Kurz, T., Pintard, L., Willis, J.H., Hamill, D.R., Gonczy, P., Peter, M., Bowerman, B., 2002. Cytoskeletal regulation by the Nedd8 ubiquitin-like protein modification pathway. Science 295, 1294–1298.

Lin, R., Thompson, S., Priess, J.R., 1995. pop-1 encodes an HMG box protein required for the specification of a mesoderm precursor in early *C. elegans* embryos. Cell 83, 599–609.

Mello, C.C., Draper, B.W., Krause, M., Weintraub, H., Priess, J.R., 1992. The pie-1 and mex-1 genes and maternal control of blastomere identity in early *C. elegans* embryos. Cell 70, 163–176.

Pellettieri, J., Seydoux, G., 2002. Anterior–posterior polarity in *C. elegans* and *Drosophila*—PARallels and differences. Science 298, 1946–1950.

Pintard, L., Kurz, T., Glaser, S., Willis, J.H., Peter, M., Bowerman, B., 2003. Neddylation and deneddylation of CUL-3 is required to target MEI-1/Katanin for degradation at the meiosis-to-mitosis transition in *C. elegans*. Curr. Biol. 13, 911–921.

Raich, W.B., Moorman, C., Lacefield, C.O., Lehrer, J., Bartsch, D., Plasterk, R.H., Kandel, E.R., Hobert, O., 2003. Characterization of *Caenorhabditis elegans* homologs of the down syndrome candidate gene DYRK1A. Genetics 163, 571–580.

Reese, K.J., Dunn, M.A., Waddle, J.A., Seydoux, G., 2000. PIE-1 localization to the germ lineage depends on two distinct mechanisms that act on separate domains in the PIE-1 protein. Mol. Cell 6, 445–455.

Rocheleau, C.E., Downs, W.D., Lin, R., Wittmann, C., Bei, Y., Cha, Y.H., Ali, M., Priess, J.R., Mello, C.C., 1997. Wnt signaling and an APC-related gene specify endoderm in early *C. elegans* embryos. Cell 90, 707–716.

Rocheleau, C.E., Yasuda, J., Shin, T.H., Lin, R., Sawa, H., Okano, H., Priess, J.R., Davis, R.J., Mello, C.C., 1999. WRM-1 activates the LIT-1 protein kinase to transduce anterior/posterior polarity signals in *C. elegans*. Cell 97, 717–726.

Rose, L.S., Kemphues, K.J., 1998. Early patterning of the *C. elegans* embryo. Annu. Rev. Genet. 32, 521–545.

Schubert, C.M., Lin, R., de Vries, C.J., Plasterk, R.H., Priess, J.R., 2000. MEX-5 and MEX-6 function to establish soma/germline asymmetry in early *C. elegans* embryos. Mol. Cell 5, 671–682.

Smith, D.J., Stevens, M.E., Sudanagunta, S.P., Bronson, R.T., Makhinson, M., Watabe, A.M., O'Dell, T.J., Fung, J., Weier, H.U., Cheng, J.F., Rubin, E.M., 1997. Functional screening of 2 Mb of human chromosome 21q22.2 in transgenic mice implicates minibrain in learning defects associated with Down syndrome. Nat. Genet. 16, 28–36.

Souza, G.M., Lu, S., Kuspa, A., 1998. YakA, a protein kinase required for the transition from growth to development in *Dictyostelium*. Development 125, 2291–2302.

Srayko, M., Buster, D.W., Bazirgan, O.A., McNally, F.J., Mains, P.E., 2000. MEI-1/MEI-2 katanin-like microtubule severing activity is required for *Caenorhabditis elegans* meiosis. Genes Dev. 14, 1072–1084.

Srinivasan, D.G., Fisk, R.M., Xu, H., Van Den Heuvel, S., 2003. A complex of LIN-5 and GPR proteins regulates G protein signaling and spindle function in *C. elegans*. Genes Dev. 17, 1225–1239.

Tabuse, Y., Izumi, Y., Piano, F., Kemphues, K.J., Miwa, J., Ohno, S., 1998. Atypical protein kinase C cooperates with PAR-3 to establish embryonic polarity in *Caenorhabditis elegans*. Development 125, 3607–3614.

Tejedor, F., Zhu, X.R., Kaltenbach, E., Ackermann, A., Baumann, A., Canal, I., Heisenberg, M., Fischbach, K.F., Pongs, O., 1995. Minibrain: a new protein kinase family involved in postembryonic neurogenesis in *Drosophila*. Neuron 14, 287–301.

Tsou, M.F., Hayashi, A., DeBella, L.R., McGrath, G., Rose, L.S., 2002. LET-99 determines spindle position and is asymmetrically enriched in response to PAR polarity cues in *C. elegans* embryos. Development 129, 4469–4481.

Tsukuba, T., Bond, J.S., 1998. Role of the COOH-terminal domains of meprin A in folding, secretion, and activity of the metalloendopeptidase. J. Biol. Chem. 273, 35260–35267.

Wallenfang, M.R., Seydoux, G., 2000. Polarization of the anterior-posterior axis of *C. elegans* is a microtubule-directed process. Nature 408, 89–92.

Zollman, S., Godt, D., Prive, G.G., Couderc, J.L., Laski, F.A., 1994. The BTB domain, found primarily in zinc finger proteins, defines an evolutionarily conserved family that includes several developmentally regulated genes in *Drosophila*. Proc. Natl. Acad. Sci. U. S. A. 91, 10717–10721.